www.czasopisma.pan.pl PAN POLSKA AKADEMIA NAUK www.journals.pan.pl

Arch. Min. Sci. **71** (2026), 1, 59-78

Electronic version (in color) of this paper is available: http://mining.archives.pl

DOI: https://doi.org/10.24425/ams.2026.157756

XINGFAN ZHANG[1,2], XIAOBO LIU[3], HONGDI JING[2*], MIAO YU[2,3], HAO WU[4]

STUDY ON INTELLIGENT OPTIMISATION SCHEME OF BENCH BLASTING PARAMETERS IN OPEN PIT

The design of blasting parameters for open-pit mines mainly relies on empirical analysis, which leads to problems such as poor blasting effect and high randomness. Conduct research on intelligent optimisation schemes for open-pit mine bench blasting parameters by combining mathematical analysis and numerical simulation methods. The specific research process mainly includes the following aspects. Based on rock mechanics experiments, obtain the mechanical parameters of ore and rock in the blasting area on-site. Constructing a prediction model for open-pit mine bench blasting and an intelligent optimisation scheme for blasting parameters based on the KUZ-RAM model. Considering the actual production of open-pit mines, and combining LS-DYNA to establish a detailed blasting simulation, a basic 3D model is used. Establish a simulation parameter scheme suitable for open-pit mine bench blasting to conduct numerical simulation research. Comparing the numerical simulation results with the actual blasting effect on site, with the goal of mining blasting fragmentation and blasting vibration, the optimisation plan for open-pit mining bench blasting parameters is verified. Practical application was carried out in Qidashan open-pit mine, a computer vision and blasting vibration analysis system was used to collect and analyse on-site data. The production operation was carried out according to the optimised hole network parameters, which significantly improved the blasting effect of Qidashan open-pit mine. The annual average cost of drilling and pyrotechnic equipment was saved by about 11.85 million yuan, verifying the feasibility and effectiveness of the research plan.

Keywords: Open pit mine; Blasting parameters; Intelligent optimization; Numerical simulation; KUZ-RAM

[1] UNIVERSITY OF SCIENCE AND TECHNOLOGY BEIJING, SCHOOL OF RESOURCES AND SECURITY ENGINEERING, BEIJING 100083, CHINA
[2] CHINESE ACADEMY OF SCIENCES, SHENYANG INSTITUTE OF AUTOMATION, SHENYANG 110016, CHINA
[3] UNIVERSITY OF SCIENCE AND TECHNOLOGY LIAONING, QIANSHANWAN MINING LABORATORY, ANSHAN 110325, CHINA
[4] NORTHEASTERN UNIVERSITY, SCHOOL OF RESOURCES AND CIVIL ENGINEERING, SHENYANG, 110819, CHINA
* Corresponding author: jinghongdi@163.com

1. Introduction

In the mining industry, blasting remains the primary method of crushing ore rock [1,2], with the proportion of rock crushed by blasting accounting for more than 90% of the total crushing volume of the mine. Blasting is the production process of open-pit mines, which involves the highest cost investment and quality requirements. The quality of blasting directly affects the productivity and cost of subsequent operations [3]. Blasting parameters are the key factors influencing the effectiveness of blasting; therefore, designing these parameters often requires a forward-looking approach. In the current state of open-pit mine production, this forward-looking mainly relies on the experience of workers [4,5], which leads to the blasting effect of high randomness and poor reliability. Qidashan open-pit mine is the largest single open-pit iron mine in Asia, with relatively fixed bench blasting parameters. The blasting parameters are difficult to adapt to changes in geological characteristics, and the blasting effect fluctuates greatly. Therefore, how to quickly and accurately form reliable blasting parameters in tight production, how to ensure blasting quality and reduce blasting costs, are urgent problems that need to be solved for such large-scale open-pit iron mines.

Many scholars have researched blast parameter optimisation. It is mainly divided into two research directions: on the one hand, it is based on the actual production blast data of mines, combined with neural network algorithms for blast effect prediction and blast parameter optimisation. Regarding blasting fragmentation, S. Farid F. Mojtahedi, Jian Zhou et al. [6,7] used the firefly algorithm to optimise an adaptive neuro-fuzzy inference system to build a prediction model for blasting lumpiness. Qiancheng Fang, Chengyu Xie et al. [2,8] further adopted the firefly algorithm to optimise networks such as GBM, SVM, GP, and ANN. The FFA-GBM model has been validated to have the highest accuracy in predicting blasting effects, using RMSE, R2, and correlation coefficient as measurement indicators. Jianyang Yu, Jimmy Aurelio Rosales-Huamani et al. [9,10] established a blasting fragmentation prediction model based on artificial neural networks from a cost perspective, and provided a quantitative decision-making basis for the rational selection of production blasting design parameters. Regarding blasting vibration, Yingui Qiu, Xiliang Zhang, et al. [11,12] improved the XGBoost model to predict the peak velocity index of the blasting mass, and then achieved the prediction of blasting vibration level. Haiqing Yang, Wei Zhu et al. [13,14] proposed a blasting vibration prediction model based on an adaptive neuro-fuzzy inference system, which can effectively solve the highly nonlinear problem. Hoang Nguyen, Sunil Kumar Bisoyi et al. [15,16] achieved prediction of blasting vibration intensity by optimising artificial neural networks. The blasting vibration was reduced by optimising the blasting parameters. Establishing an intelligent prediction model for bench blasting effect requires a large amount of mining production data with good generalisation as support. However, the blasting parameters in mining production are relatively fixed, making it difficult to meet the training requirements of neural networks. Concurrently, the number of blasting operations in mines is limited each year, and obtaining a large amount of mining blasting data is also difficult. As a result, there are significant limitations in using neural networks to predict blasting effects and optimise blasting parameters.

On the other hand, the blasting process is simulated in the form of numerical calculation to achieve the purpose of predicting the blast effect and optimising the design scheme. Regarding blasting vibration, Rangang Yu et al. [17] used the particle expansion loading algorithm of the PFC program for numerical analysis of rock blasting, and verified the reliability of simulating the

blasting vibration effect in the peripheral area. Li He et al. [18] established a 3D finite element simulation model of slopes and tunnels, and analysed the vibration response characteristics of the slope surrounding rock. A mathematical model for predicting peak particle velocity based on dimensional analysis theory was established, which improved the accuracy of predicting peak particle velocity on slope surfaces. Regarding blasting fragmentation, Liu Yang et al. [19] used a finite-discrete element coupling method to systematically study the effects of borehole inclination angle on the blasting process, the evolution of damage and energy, and the state of flying stone. M. Lak, Xiaofeng Hu et al. [20,21] proposed a 3D reconstruction method for jointed rock masses, which was used for blasting simulation, fully revealing the dynamic response and blasting damage characteristics of jointed rock masses. Previous numerical simulation and theoretical analysis methods for bench blasting mainly relied on one-way verification of parameter rationality. Continuously adjust parameters to revalidate their rationality. This method is relatively inconvenient for practical application in mining sites. This approach is impractical for application in mine sites. Consequently, this paper proposes an alternative approach. It utilises in situ rock samples obtained from an open-pit mine site to determine the mechanical parameters of mine rock in the blast area. It employs the KUZ-RAM model to establish a prediction model and a parameter optimisation scheme for open-pit mine bench blasting effects. Establish the blasting simulation model using LS-DYNA and conduct detailed numerical simulation research. Targeting the distribution of blasting fragmentation and blasting vibration, achieve precise and intelligent optimisation of blasting parameters. This study can greatly improve the production efficiency of mine blasting parameter design work, as well as the scientificity and accuracy of blasting parameter design.

2. Technical principles of the programme

This paper proposes an intelligent optimisation scheme for the blasting parameters of open-pit mine steps. The Qidashan open-pit mine is used as a case study, and a prediction model for open-pit mine bench blasting is constructed. The specific research contents are as follows:

Firstly, samples of the ore rock body in the target mine to be blasted are collected, and the basic rock mechanics information of the target area is obtained through indoor rock mechanics experiments. The results of the rock mechanics experiments in the target area are then used as the input parameters of the KUZ-RAM model. The fragmentation distribution is predicted under different borehole network parameters, with the requirements of the drilling rigs' construction precision in open-pit mines taken into account. The results of the optimisation of the blast parameters of the bench blasting are determined preliminarily. Secondly, to further verify the reasonableness of the optimised blasting parameters, a fine simulation model of the target blast zone is established by combining the mechanical data of the real mining rock body obtained from the rock mechanics experiment, and the simulation of the bench blasting process in open-pit mines is carried out based on LS-DYNA, with the focus on the analysis of the two indexes of the blasting bulkiness and the blasting vibration. Finally, the effectiveness of the overall scheme of intelligent optimisation of blasting parameters is verified by means of field experiments. The outcomes demonstrate that the technical solutions conceptualised in this study are capable of attaining the objective of optimising blasting parameters and enhancing the overall efficacy of blasting operations. This provides a theoretical and technical foundation for the optimisation of bench blasting solutions in large open-pit mines.

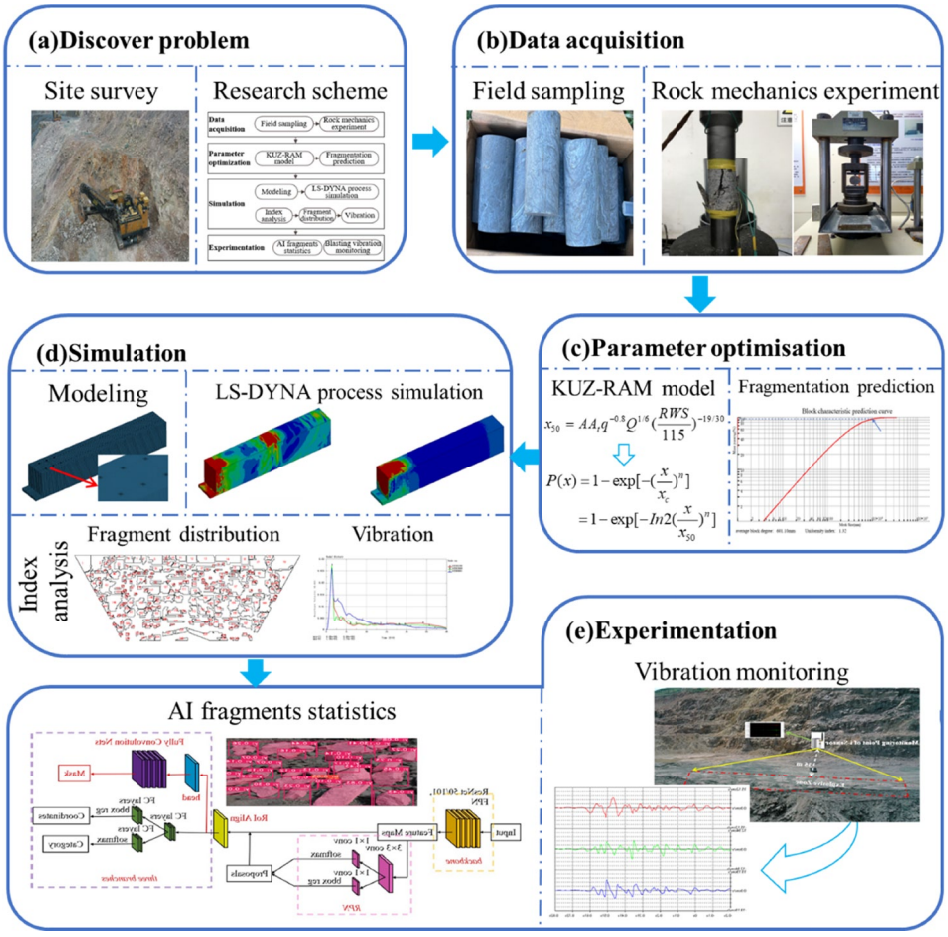

Fig. 1. Technical route

3. Mechanical parameters of ore rock

3.1. Rock specimen collection

The Qidashan open-pit mine is located 12 km northeast of Anshan City, which is the largest open-pit iron ore mine in Asia, with more than 1,000 times of bench blasting per year. The focus of this paper is the Qidashan open-pit mine, specifically the –120 m to –105 m horizontal blast area, with a section height of 15 m, a blasting bench width ranging from 20 m to 28 m, a slope angle of 65°, a hole diameter of 0.25 m, and a hole depth of 17.5 m. The blasting method employed is hole-by-hole detonation.

In order to obtain the standard specimens required for the indoor rock mechanics tests, the core was randomly sampled and processed at Qidashan quarry. The site conditions and specimen processing results at Qidashan are shown in Fig. 2.

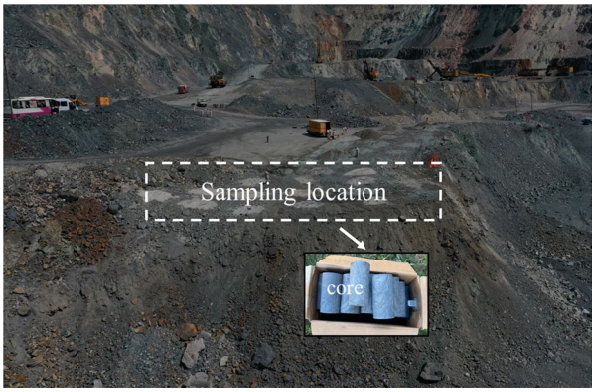

Fig. 2. On-site sampling and processing

3.2. Rock mechanics experiment

In accordance with the prevailing standards for engineering rock testing, the standard specimens were subjected to a dual processing procedure, in accordance with the stipulated requirements for uniaxial compressive strength, Brazilian split tensile strength and shear strength tests. The basic parameters of each specimen were measured and recorded with vernier callipers, an electronic balance, an ultrasonic tester and a digital camera.

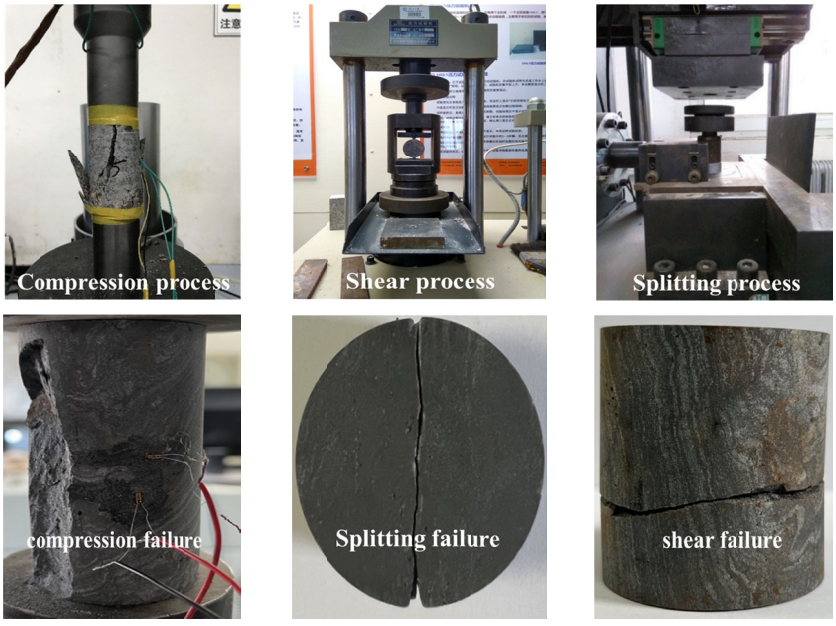

(a) Uniaxial compression test (b) Brazilian disc test (c) Straight Shearing Test

Fig. 3. Laboratory rock mechanics experiment

The following rock mechanical parameters were obtained through the acquisition of in situ specimens (as shown in Fig. 2) and indoor rock mechanics experiments (as shown in Fig. 3): the uniaxial compressive strength of the open specimen ranged from 248.08 MPa to 348 MPa. The modulus of elasticity ranged from 41.12 MPa to 78.55 MPa, the tensile strength ranged from 15.26 MPa to 18.78 MPa, the Poisson's ratio ranged from 0.18 to 0.21, and the measured average cohesion of the area is 22.87 MPa, and the average internal friction angle is 36.67°. The mean values of each mechanical parameter of the in-situ mineral rock specimens are displayed in TABLE 1.

TABLE 1

Average value of mechanical parameters of ore and rock samples

Elastic modulus (GPa)	Poisson's Ratio	Compressive strength (MPa)	Cohesion (MPa)	Internal friction angle (°)	Tensile strength (MPa)
59.83	0.20	294.46	22.87	36.67	15.95

4. Optimisation of blasting parameters

The initial KUZ-RAM model was proposed by Kuznetsov [22], and Cunningham [23] subsequently proposed a new KUZ-RAM prediction model by combining the Kuznetsov model and the Rosin-Rammler distribution function.

In this section, the optimisation of blasting parameters will be achieved based on the basic condition parameters of the ore rock in combination with the KUZ-RAM prediction model. The optimised parameters of the bench blast hole network can provide fundamental data support for the purposes of blast simulation and validation studies.

4.1. Predictive modelling of blasting effects

The quantitative relationship between the blasting parameters (including hole network parameters, charge parameters, rock characteristics, etc.) and the blasting block information is established by the KUZ-RAM model as follows:

$$P(x) = 1 - \exp\left[-\left(\frac{x}{x_c}\right)^n\right] = 1 - \exp\left[-In2\left(\frac{x}{x_{50}}\right)^n\right] \tag{1}$$

Where x_{50} is the average fragmentation size, mm; n is the homogeneity index; x_c is the characteristic grain size, mm.

(1) The calculation formula for the x_{50} value is as follows:

$$x_{50} = AA_t q^{-0.8} Q^{1/6} \left(\frac{RWS}{115}\right)^{-19/30} \tag{2}$$

Where A is the rock action index; A_t is the delay time action index; q is the unit consumption of explosives, kg/t; Q is the single-hole charge, kg; RWS is the equivalent action strength of explosives.

The formula for the rock action index A is as follows:

$$A = 0.06 \times (RMD + RDI + HF + JF) \times C(A) \tag{3}$$

Where RMD is the rock hardness condition index, in which powdery friable rock takes the value of 10, and complete rock takes the value of 50; RDI is the rock density influence index, $RDI = 25\rho - 50$; HF is the rock strength influence index, when $E < 50$ GPa, $HF = E/3$, when $E > 50$GPa, $HF = \sigma_c/5$; $JF = JPS + JPA$, JPS is the rock mass degree of completion index, take the value of 10~20, JPA is the dip influence index, take the value of 20~40; $C(A)$ is the adjustment parameter, usually take the value of 1.

The formula for A_t is as follows [24]:

$$A_t = \begin{cases} 0.66\left(\dfrac{\Delta T}{T_{\max}}\right)^3 - 0.13\left(\dfrac{\Delta T}{T_{\max}}\right)^2 - 1.58\left(\dfrac{\Delta T}{T_{\max}}\right) + 2.1, & \dfrac{\Delta T}{T_{\max}} \le 1 \\ 0.9 + 0.1\left(\dfrac{\Delta T}{T_{\max}} - 1\right), & \dfrac{\Delta T}{T_{\max}} > 1 \end{cases} \tag{4}$$

$$T_{\max} = \frac{15.6}{c_p} B \tag{5}$$

Where ΔT is the inter-hole delay time, s; B is the resistance line, m; c_p is the p-wave velocity, m/s.

(2) n is calculated as follows:

$$n = n_s \left(2 - 0.03\frac{B}{d}\right)^{0.5} \left(\frac{1 + S/B}{2}\right)^{0.5} \left(1 - \frac{W}{B}\right) \left(\frac{L_c}{H}\right)^{0.3} \left(\frac{A}{6}\right)^{0.3} C(n) \tag{6}$$

Where d is the diameter of the hole, m; S is the hole distance, m; W is the drilling deviation, m; L_c is the length of the charge, m; H is the height of the bench, m; $C(n)$ is the adjustment parameter; n_s is the detonator-related parameter.

4.2. Intelligent optimisation of blasting parameters

In order to facilitate the application of field technicians, a prediction model has been developed for the intelligent prediction of blasting effect and the intelligent optimisation procedure of blasting parameters for open pit mines. This model is based on rock condition parameters and hole network parameters, with the aim of achieving intelligent prediction of the distribution of blasting fragmentation.

Mines can utilise their specific bench blasting hole pattern parameters, rock mechanics parameters, and rock mass structural parameters, among others, as system inputs to predict blasting outcomes. Additionally, by conducting comprehensive geological surveys, mines can categorise rock mass strength and fracture zones, thereby establishing a database of rock strength and structural features within the mine. Fuzzy assessments of rock strength and structural characteristics, based on the location of the blasting area, are employed as input parameters for the system.

As illustrated in Fig. 4 below, the horizontal axis of the blasting effect prediction curve is the fragmentation, and the vertical axis is the block passing rate.

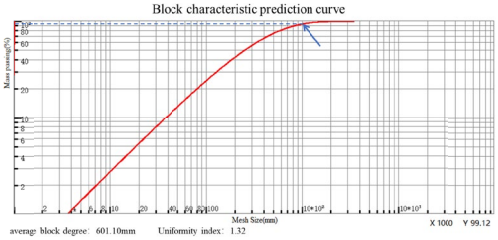

(a) Fragmentation size prediction curve of 6×7 m

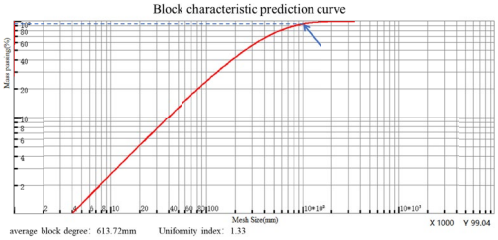

(b) Fragmentation size prediction curve of 6×7.5 m

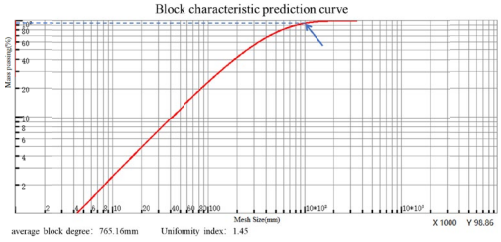

(c) Fragmentation size prediction curve of 8×6 m

Fig. 4. Prediction results of blasting effect

The current parameters of the Qidashan open-pit mine's hole network are as follows: hole spacing of 7 m, row spacing of 6m, blast hole diameter of 250 mm, stemming length of 5 m, hole depth of 17.5 m, resistance line ranging from 3.5 m to 5 m, inter-hole delay time of 25 ms, designed unit consumption of 0.41 kg/t, bench height of 15 m, charging height of 10m, and single-hole charge weight varying between 670 kg and 730 kg. The rock parameters include a rock density of 3310-3517 kg/m^3, compressive strength ranging from 62.02 MPa to 97.24 MPa, tensile strength from 7.26 MPa to 9.39 MPa, elastic modulus between 50.28 GPa and 69 GPa, Poisson's ratio of 0.18-0.21, cohesion of 5.69-7.37 MPa, and internal friction angle ranging from 48.53° to 51.67°. Characteristics of the rock mass structural planes are as follows: intact rock mass with RMD = 50, nearly horizontal rock fissures with JPA = 10, tightly combined rock mass with JCF = 1, and structural planes larger than 0.1 m with JPS = 20-50. Based on the outcomes of the intelligent prediction and dynamic parameter optimisation system for blasting fragmentation in open-pit mines, blasting optimisation is conducted in conjunction with the aforementioned parameters.

Blasting optimisation can be accomplished through adjustments to the detonation method and sequence, type of explosive, blast hole arrangement, and hole network parameters, while taking into account the practicality of mining operations [25]. This article optimizes the scheme by modifying the hole spacing. Considering the construction precision of the rotary drilling rig at the site and the production demands of the mine, the hole spacing is adjusted in increments of 0.5 m, and the corresponding blasting effect prediction curve is generated.

After blasting, loading, transporting, and crushing, the ore from Qidashan open-pit mine is dispatched to external locations. Following an on-site tracking investigation, it was found that the

electric shovel used is the WK-10B (with a bucket capacity of 10-16 m^3), the mining truck is the NTE200 (with a loading volume of 92-123 m^3), and the crusher is the PE-1200×1500 (capable of handling feed material with a maximum block size of 1020 mm). The primary factor restricting the ore size is the feed block size of the crusher. The PE-1200×1500 crusher features a feed opening size of 1200×1500 mm, a maximum feed particle size of 1020 mm, and an adjustable feed opening range of 150-300 mm. Taking into account the current production scenario and incorporating a degree of production redundancy, ores with a length exceeding 1m or a maximum cross-sectional area exceeding 0.8 m^2 are classified as large blocks. The optimised drilling pattern parameters and block size prediction results are presented in TABLE 2.

TABLE 2

Optimisation parameters and prediction results

Plan	Pitch (m)	Array pitch (m)	Section height (m)	Boulder yield (%)	Average fragmentation size (mm)
Plan 1	7.0	6.0	15	0.88%	601.10
Plan 2	7.5	6.0	15	0.96%	613.72
Plan 3	8.0	6.0	15	1.14%	765.16

Taking the financial implications into consideration, it can be concluded that option 2 is the most suitable solution. The original scheme 1 predicted a bulk rate of 0.88% and an average fragmentation size of 601.10 mm. When the scheme 2 hole spacing increased to 7.5 m, the blasting bulk rate increased by only 0.08% and the average fragmentation size increased by only 12.62 mm. However, when the scheme 3 hole spacing increased to 8 m, the predicted value of the bulk rate and the average fragmentation size increased dramatically. It is evident that the considerable escalation in both the bulk rate and the mean fragmentation size will result in a subsequent reduction in the efficiency of shovel loading and transport operations. This, in turn, will precipitate an increase in the cost of secondary blasting. However, it is anticipated that the hole spacing of 7.5 m and the row spacing of 6 m of the hole network parameters, in accordance with the prevailing operating conditions on site, will optimise the process.

5. Blast simulation verification

It is evident that the implementation of reasonable blasting parameters can effectively enhance mine production efficiency. In the preceding section, the optimised bench blasting hole network parameters were obtained. In this section, numerical calculations will be employed to conduct a blasting simulation. This will involve the optimised blasting parameter scheme, with the objective of verifying the reliability of the optimisation of blasting parameters.

5.1. Numerical modelling of bench blasting

In order to ensure the accuracy of the calculation and to expedite the simulation process, the area to be blown up was combined with the model size of 60 m×25 m×20 m. The ore body was configured with three rows of gun holes, with a spacing of 7.5 m between the holes, 6.0 m between the rows, and a diameter of 0.25 m for each hole. The depth of the holes was set

at 17.5 m, and the gun hole filling was taken into account in the design. The eight-node hexahedral cell SOLID164 is utilised to mesh the calculation model, and the number of model cells is 507600. The parameters to be set include the blasting detonation point, the detonation time and differential time in addition to other parameters. Rock fractures are among the factors influencing rock strength and blasting efficiency [26]. However, since the blasting area is relatively small, large-scale fracture structures are typically absent. The characteristics of small-scale fractures within the rock mass of the bench can be accounted for through strength reduction. To enhance the applicability of the model, the impact of fracture structures is not taken into consideration in the simulation model of this study.

The blasting zones in open-pit mine benches are predominantly trapezoidal in shape, as illustrated in Fig. 5. Among these, faces 1, 2, and 3 constitute the exposed free surfaces, whereas faces 4, 5, and 6 are contiguous with the ore body. During the model construction process, the free surfaces of the blasting zone are designated as free boundary conditions. Instead of assigning specific values to the solution at the boundary, the behaviour of the solution on the boundary is governed by natural phenomena or physical laws, thereby enabling the simulation of the stress wave's dynamic state upon reaching the free surface with utmost fidelity. The interface in contact with the ore body is configured with a non-reflective boundary condition to emulate the infinite rock mass environment surrounding the blasting zone. This non-reflective boundary condition minimises the reflection effect of the blast wave, thereby ensuring the accuracy and reliability of the computational results.

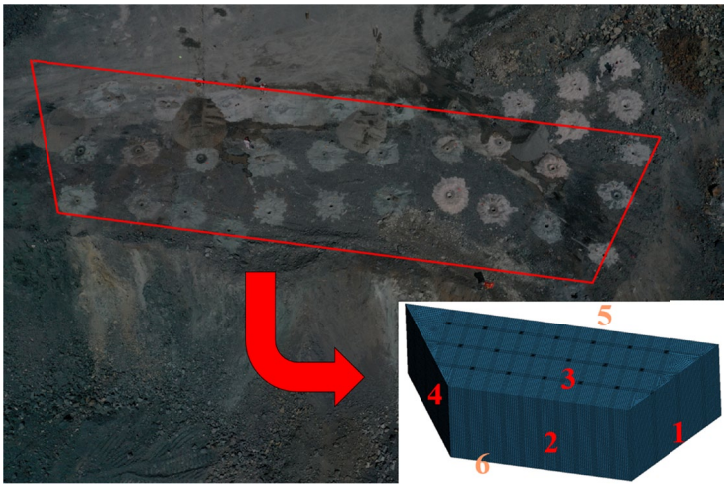

Fig. 5. Blasting simulation model

Rock blasting is an extremely complex process of energy transfer and dissipation, and the use of numerical models can accurately describe the dynamic response of rock during blasting. The RHT model (as shown in TABLE 3) employed in this study is an intrinsic model for describing the dynamic mechanical behaviour of brittle materials, such as concrete, proposed by Riedel, Hiermaier and Thoma [27], which is suitable for analysing the complex dynamic mechanical processes of rock comminution, rupture and damage under blasting loading conditions [28].

TABLE 3

RHT model parameters

G/MPa	A_1/GPa	A_2/GPa	A_3/GPa	A	N	A_f
24929.7	64.74	90.64	33.66	1.6	0.61	1.6
N_f	D_1	D_2	β_0^c/ms^{-1}	β_0^t/ms^{-1}	β^c/ms^{-1}	β^c/ms^{-1}
0.61	0.04	1	3.0×10^{-8}	3.0×10^{-9}	3.0×10^{22}	3.0×10^{22}

The parameters of the blasting materials utilised are delineated in TABLE 4.

TABLE 4

Blasting material parameters

ρ_e/kg·m^{-3}	D/m·s^{-1}	P_{cj}/GPa	A/GPa	B/GPa	R_1	R_2	E_0/MJ·m^{-3}	ω
1150	5122	9.53	276.2	8.44	5.199	2.099	3870	0.33

5.2. Analysis of bench blasting results

5.2.1. Analysis of fragmentation in bench blasting

The numerical simulation of damage results has been analysed, with the analysis method combining Image J with a step crushing block degree analysis. As illustrated in Fig. 6(a) and Fig. 6(c), the bench blast x-z and y-z damage profile is removed, and the blast damage region can be obtained in Fig. 6(b) and Fig. 6(d) below the profile block degree map.

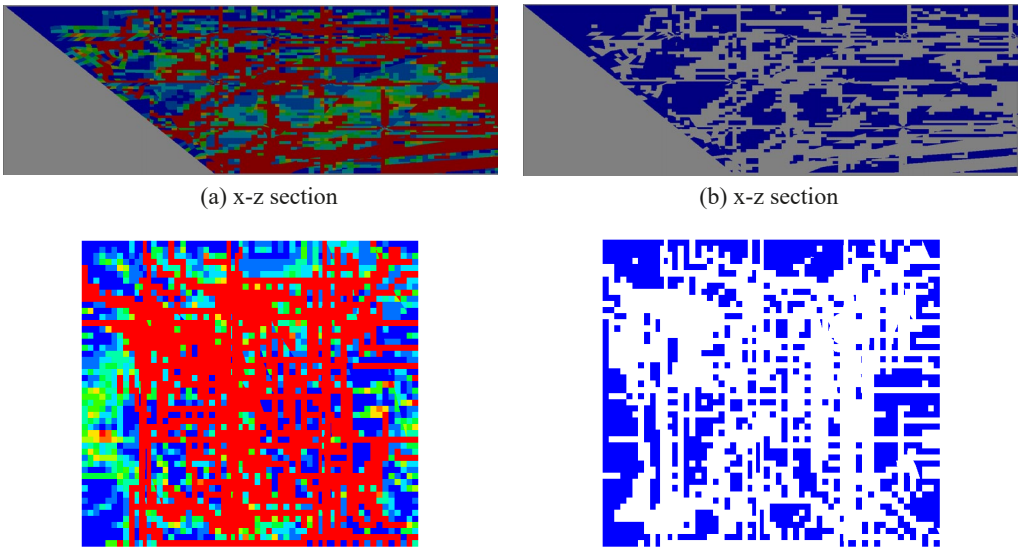

(a) x-z section (b) x-z section

(c) y-z section (d) y-z section

Fig. 6. Blasting damage profile

In the analysis process, firstly, the relevant parameters of Image J should be set, secondly, the non-fragmented areas should be covered with colour blocks, and finally, the corresponding blast block degree of the step profile should be counted by Image J.

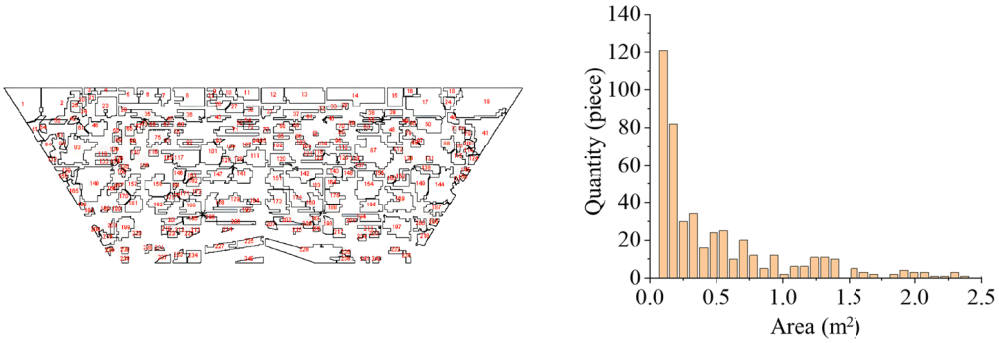

a) Block division (b) Fragment distribution

Fig. 7. Blasting fragmentation distribution of x-z profile

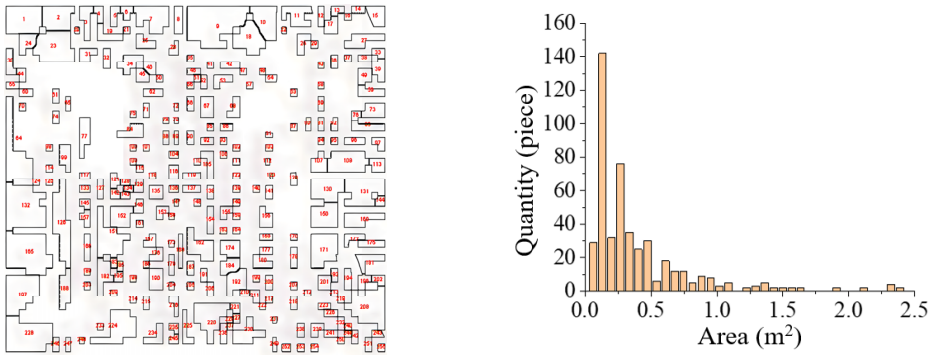

(a) Block division (b) Fragment distribution

Fig. 8. Blasting fragmentation distribution of y-z profile

As illustrated in Fig. 7, the number of particles in the x-z profile is 494, and as demonstrated in Fig. 8, the number of particles in the y-z profile is 511. The specific fragmentation size distribution results are displayed in the above figure. From the fragmentation size distribution histogram, it can be observed that the majority of the blasting fragmentation area is concentrated in 0.5 m^2 or less. In conjunction with the profile, it is evident that the large blocks are predominantly concentrated at the edge of the steps.

In accordance with the stipulated criteria for the subsequent processes of shovelling and transportation in the Qidashan open-pit mine, ore rocks exhibiting a cross-sectional area in excess of 0.8 m^2 are designated as massive. The results of the aforementioned analysis demonstrate that the bulk rate obtained from the x-z profile calculation is 1.0%, and the bulk rate obtained from the y-z profile calculation is 0.9%. The blasting parameter intelligent optimisation system

predicts that the final preferred option 2 has a bulk rate of 0.96, which is between the two, and the difference is relatively small. This verifies the intelligent optimisation of the system and the accuracy of the prediction results.

5.2.2. Analysis of Vibration in bench blast

The dimensions of the bench blasting calculation model are 15 m×112 m×20 m. The ore body is comprised of three rows, totalling six blasting holes. The model takes into account micro-differential blasting between the holes. The finite element calculation model is shown in Fig. 9.

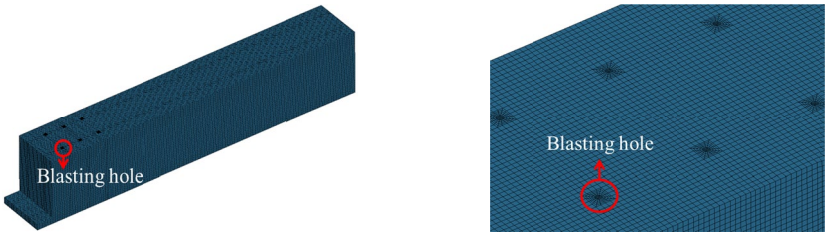

(a) Model mesh division (b) Blast hole area grid

Fig. 9. Calculation model of blasting vibration

The seismic effect produced by blasting is the result of several factors, including the location of the blast source, the amount of explosives, the blasting method and the geological conditions traversed in the propagation process, etc. The seismic wave formed by blasting is the primary cause of engineering blasting hazards [29,30]. When integrated with the actual parameters of the mine, the blasting vibration simulation can generate a variety of velocity cloud diagrams, as illustrated in Fig. 10.

The maximum vibration speeds in the x, y and z directions and the combined vibration speeds at the surface monitoring points at 35 m, 65 m and 100 m from the center of explosion are shown in TABLE 5.

TABLE 5

Simulated blasting vibration information

Distance from the explosion center	Maximum vibration velocity in x-direction	Maximum vibration velocity in y-direction	Maximum vibration velocity in z-direction	Maximum combined vibration speed
35 m	6.24 cm/s	7.48 cm/s	8.33 cm/s	9.52 cm/s
65 m	4.11 cm/s	2.06 cm/s	2.34 cm/s	4.52 cm/s
100 m	2.33 cm/s	1.55 cm/s	1.45 cm/s	2.4 cm/s

From the above results, it can be observed that the blasting vibration spreads from the borehole to the surrounding area. The energy loss increases with the increase in distance from the blast centre. At the middle position of the model, there is a vertical increase in vibration velocity, which is mainly caused by the superposition effect of micro-difference blasting vibration

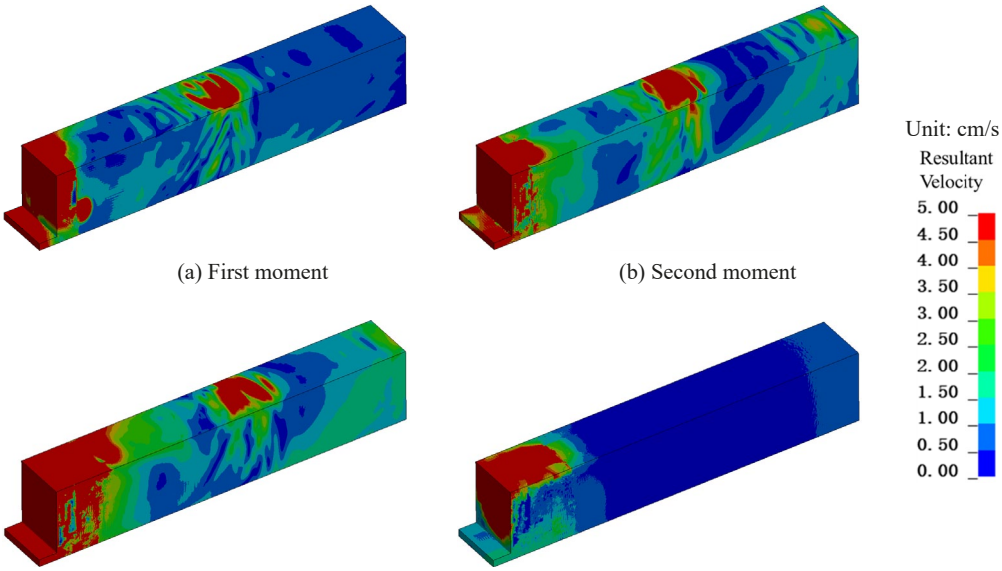

(a) First moment (b) Second moment

(c) Third moment (d) Fourth moment

Fig. 10. Combined vibration velocity distribution during blasting

in the middle and far regions. However, as the monitoring point at 65 m is situated at a greater distance from the blast centre, the amplitude of vibration velocity attenuation caused by blasting energy loss is much greater than the vibration velocity change caused by the superposition effect of blasting vibration stress waves. Consequently, the maximum vibration velocity value recorded at 65 m is still lower than that measured at 35 m. According to the simulation results of blasting vibration, the maximum combined velocity of blasting vibration is 9.63 cm/s, which meets the requirements of the „Blasting Safety Regulations" for the allowable value of blasting vibration velocity. It verifies the rationality of the optimisation plan from a safety perspective.

6. Field experimental verification

Based on the results of intelligent optimisation of bench blasting parameters in open pit mines, field experiments were carried out on the 31st bench blasting in Qidashan open-pit mine at –120 m to –105 m level. The optimized hole network parameters: hole spacing of 7.5m, row spacing of 6m, blast bench width of 20 m-28 m, step area of 3168 m^2, total volume of 47520 m^3, rock volume of 104664 t, the use of hole-by-hole detonation, the gun hole diameter of 0.25 m, the gun hole depth of 17.5 m, the overburden depth of 2.5 m, and the type of explosives are emulsified and ammonium oil explosives.

After the bench blasting, the Mask R-CNN network is used to construct an image segmentation-based ore chunk detection and statistical model, and the threshold of large ore cut-off area is set to 0.8 m^2. A total of 960 photographs of the blasting site were collected, of which 900 are the training set, and 60 are the test set. The model training parameters are shown in TABLE 6, and the results of ore chunk detection at the blast site of open pit mines are shown in Fig. 11.

TABLE 6

Test model training parameters

Parameter Type	Parameter values
Resolution	550×550
imgs_train	900
batch_szie	10
epochs	50

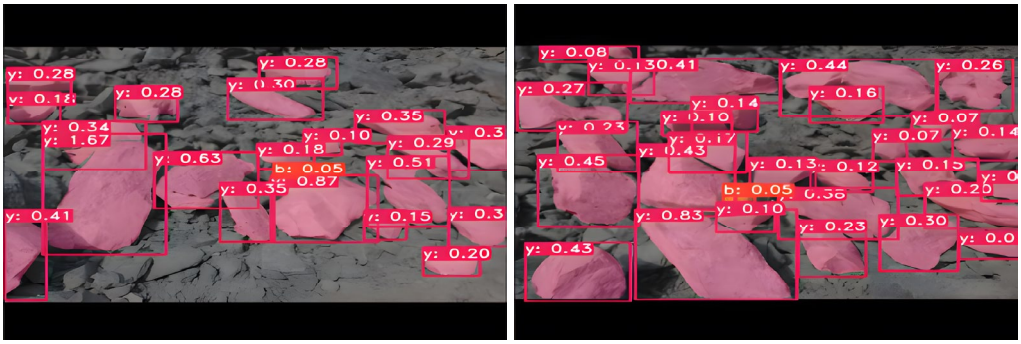

(a) Local testing results

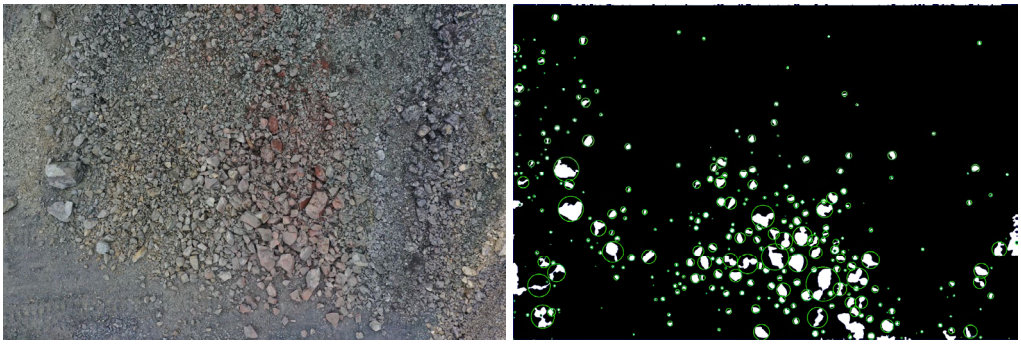

(b) Overall testing results

Fig. 11. Test results of bursting fragmentation

According to statistics, the site blasting effect is good, did not see a significant increase in large blocks, the blasting pile is in good shape, no root, blasting block rate of 0.93%, and the intelligent optimisation system prediction, numerical simulation results are similar to meet the mine production requirements.

As shown in Fig. 12, the permanent embankment near the blasting area of the open pit mine is selected as the monitoring object, the *i*-Sensor sensor is placed, and the characteristic data is analysed using the imsServer blast vibration analysis system. Taking the monitoring point at 35 m closest to the blast centre as an example, the monitoring results are shown in TABLE 7.

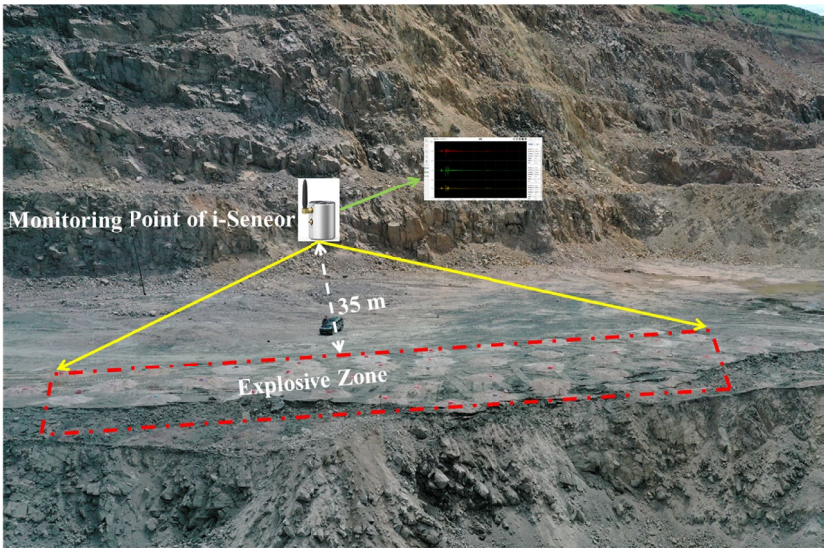

Fig. 12. Monitoring and analysis of blasting vibration based on *i*-Sensor

TABLE 7

Blasting vibration data of monitoring points at 35 m

Channel	Maximum vibration speed (cm/s)	Main vibration frequency (Hz)	Duration (s)
1	7.561	10.986	0.773
2	–6.469	14.648	0.803
3	9.595	109.86	0.691

As demonstrated in TABLE 5 and TABLE 7, the peak velocity of the monitoring data at 35 m from the burst centre exhibits a high degree of correlation with the simulation results.

Utilising the research methodology outlined in this paper, numerous experiments were conducted in various production zones of the Qidashan Open-Pit Mine to gather statistical data on blasting fragmentation and blasting vibration indicators. The outcomes of these experiments are presented in TABLE 8.

Calculate the root mean square error (RMSE) and coefficient of determination (R^2) for the bulk rate and blasting vibration indicators, utilising both the simulation results from the statistical program and the on-site monitoring data.

$$RMSE = \sqrt{\sum_{j=1}^{N_1} \frac{\left(E_j - P_j\right)^2}{N_1}} \tag{7}$$

$$R^2 = 1 - \frac{\sum_{j=1}^{N_1} \left(P_j - E_j\right)^2}{\sum_{j=1}^{N_1} \left(E_j - E\right)^2} \tag{8}$$

TABLE 8

Blasting effect statistics

Blasting area	Hole spacing (m)	Row spacing (m)	Simulation results		Monitoring results	
			Boulder yield (%)	Peak vibration velocity (cm/s)	Boulder yield (%)	Peak vibration velocity (cm/s)
–105 m level The 31st blasting	7.5	6.0	1.16	8.86	1.23	8.92
–-105 m level The 23rd blasting	7.5	6.0	1.03	9.57	0.99	9.61
–105 m level The 25th blasting	7.5	6.0	1.02	9.13	1.05	9.05
–105 m level The 29th blasting	7.5	6.0	0.93	9.25	0.96	9.31
–120 m level The 16th blasting	7.0	6.0	0.95	8.86	0.98	9.15
–120 m level The 18th blasting	7.0	6.0	1.09	8.95	1.13	8.78
–120 m level The 20th blasting	7.0	6.0	0.91	10.05	0.89	10.26
–135 m level The 9th blasting	6.5	6.0	0.99	10.01	0.95	9.95
–135 m level The 5th blasting	6.5	6.0	0.89	9.97	0.89	10.08
–135 m level The first blasting	6.5	6.0	1.16	8.86	1.23	8.92

After calculation, the RMSE value of the block rate indicator is 0.04, and theR^2 value is 0.91; The RMSE value of the blasting vibration index is 0.14, and the R^2 value is 0.92.

In summary, through multiple bench blasting experiments on site, it can be observed that the fragmentation size and vibration indicators from blasting are closely aligned with both predictive and simulation results, meeting the production requirements of the mining operation. The root mean square error (RMSE) values for blockiness and blasting vibration indicators are relatively low, while the R^2 values remain above 0.9. The results from field experiments validate the effectiveness and reliability of the intelligent optimisation scheme for open-pit mine bench blasting parameters.

7. Conclusions

The present paper focuses on the poor timeliness of traditional open-pit mine bench blasting parameter optimisation, and on the research of an intelligent optimisation scheme for bench blasting parameters in large open-pit iron ore mines. Utilising rock mechanics experiments, the mechanical parameters of mine rock under real environmental conditions in the field were obtained. The KUZ-RAM model was employed to construct a prediction model for bench blasting and an intelligent optimisation scheme for blasting parameters of open-pit mines. A blasting simulation model conforming to the actual working conditions in the field was established to

carry out numerical simulation and verification of the optimised bench blasting parameters. The reliability and effectiveness of the optimisation scheme were further verified by the on-site experiment in the open-pit mine of Qidashan. The reliability and validity of the optimisation scheme are further verified by field experiments in the Qidashan open-pit mine. The following conclusions are drawn from this study:

(1) A prediction model of bench blasting in open pit mines is obtained based on the KUZ-RAM model, and an intelligent optimisation program of blasting parameters in open pit mines is developed, which realises intelligent prediction of the distribution of blasting blocks and rapid optimisation of blasting parameters.

(2) The effectiveness and reasonableness of the optimisation programme are verified from the perspectives of blasting effect and blasting safety, based on the results of LS-DYNA blasting simulation.

(3) The optimised large-hole network parameters are used to carry out bench blasting experiments in the open-pit mine site, and the intelligent evaluation of the blasting effect in the site is completed based on Mask-RCNN. The results of the study demonstrate that the drilling and blasting efficiency is not only significantly enhanced under the premise of guaranteeing the quality of the blasting, but also reduces the production cost.

Acknowledgements

This work is financially funded by the Project (52474172&U21A20106) Supported by the Research Fund of National Natural Science Foundation of China.

References

[1] Z. Yu, X.Z. Shi, Z.X. Zhang, Y.G. Guo, X.H. Miao, I. Kalipi, Numerical Investigation of Blast-Induced Rock Movement Characteristics in Open-Pit Bench Blasting Using Bonded-Particle Method. Rock. Mech. Rock. Eng. **55** (6), 3599-619 (2022). DOI: https://doi.org/10.1007/s00603-022-02831-w

[2] Q.C. Fang, H. Nguyen, X.N. Bui, T. Nguyen-Thoi, J. Zhou, Modeling of rock fragmentation by firefly optimization algorithm and boosted generalized additive model. Neural. Comput. Appl. **33** (8), 3503-19 (2020). DOI: https://doi.org/10.1007/s00521-020-05197-8

[3] Z.Z. Zhang, R.X. Zhang, J.D. Sun, X.F. Xu, Y.B. Tao, S.K. Lv, Study on the Determination Method of Cast Blasting Stockpile Forms in an Open-Pit Mine. Lect. Notes. Comput. Sc. **12** (13) (2022). DOI: https://doi.org/10.3390/app12136428

[4] X.H. Ding, K.M. Li, S.S. Xiao, W.M. Hu, Analysis of key technologies and development of integrated digital processing system for cast blasting design. J. Cent. South. Univ. **22** (3), 1037-44 (2015). DOI: 10.1007/s11771-015-2614-7

[5] A. Baetin, O. Zta, A.I. Kanli, EQS: A computer software using fuzzy logic for equipment selection in mining engineering. J. S. Afr. I. Min. Metall. **106** (1), 63-70 (2006).

[6] S.F.F. Mojtahedi, I. Ebtehaj, M. Hasanipanah, H. Bonakdari, H.B. Amnieh, Proposing a novel hybrid intelligent model for the simulation of particle size distribution resulting from blasting. Eng. Comput. **35** (1), 47-56 (2018). DOI: https://doi.org/10.1007/s00366-018-0582-x

[7] J. Zhou, C.Q. Li, C.A. Arslan, M. Hasanipanah, H.B. Amnieh, Performance evaluation of hybrid FFA-ANFIS and GA-ANFIS models to predict particle size distribution of a muck-pile after blasting. Eng. Comput. **37** (1), 265-74 (2019). DOI: https://doi.org/10.1007/s00366-019-00822-0

[8] C.X. Xie, H. Nguyen, X.B. Bui, Y. Choi, J. Zhou, T. Nguyen-Trang. Predicting rock size distribution in mine blasting using various novel soft computing models based on meta-heuristics and machine learning algorithms. Geosci. Front. **12** (3), (2021). DOI: https://doi.org/10.1016/j.gsf.2020.11.005

[9] J.Y. Yu, S.J. Ren, Prediction and Analysis Method of Mine Blasting Quality Based on GA-BP Neural Network. Mob. Inf. Syst. **2022**, 1-8 (2022). DOI: https://doi.org/10.1155/2022/9239381

[10] J.A. Rosales-Huamani, R.S. Perez-Alvarado, U. Rojas-Villanueva, J.L. Castillo-Sequera, Design of a Predictive Model of Rock Breakage by Blasting Using Artificial Neural Networks. Symmetry-basel. **12** (9) (2020). DOI: https://doi.org/10.3390/sym12091405

[11] Y.G. Qiu, J. Zhou, M. Khandelwal, H.T. Yang, P.X. Yang, C.Q. Li, Performance evaluation of hybrid WOA-XGBoost, GWO-XGBoost and BO-XGBoost models to predict blast-induced ground vibration. Eng. Comput. **38** (S5), 4145-62 (2021). DOI: https://doi.org/10.1007/s00366-021-01393-9

[12] X.L. Zhang, H. Nguyen, X.N. Bui, Q.H. Tran, D. Nguyen, D.T. Bui, H.A. Moayedi, Novel Soft Computing Model for Predicting Blast-Induced Ground Vibration in Open-Pit Mines Based on Particle Swarm Optimization and XGBoost. Nat. Resour. Res. **29** (2), 711-21 (2019).
DOI: https://doi.org/10.1007/s11053-019-09492-7

[13] H.Q. Yang, M. Hasanipanah, M.M. Tahir, D.T. Bui, Intelligent Prediction of Blasting-Induced Ground Vibration Using ANFIS Optimized by GA and PSO. Nat. Resour. Res. **29** (2), 739-50 (2019).
DOI: https://doi.org/10.1007/s11053-019-09515-3

[14] W. Zhu, H.N. Rad, M. Hasanipanah, A chaos recurrent ANFIS optimized by PSO to predict ground vibration generated in rock blasting. Appl. Soft. Comput. **108** (2021). DOI: https://doi.org/10.1016/j.asoc.2021.107434

[15] H. Nguyen, X.N. Bui, A Novel Hunger Games Search Optimization-Based Artificial Neural Network for Predicting Ground Vibration Intensity Induced by Mine Blasting. Nat. Resour. Res. **30** (5), 3865-80 (2021).
DOI: https://doi.org/10.1007/s11053-021-09903-8

[16] Y.H. Shang, H. Nguyen, X.N. Bui, Q.H. Tran, H. Moayedi, A Novel Artificial Intelligence Approach to Predict Blast-Induced Ground Vibration in Open-Pit Mines Based on the Firefly Algorithm and Artificial Neural Network. Nat. Resour. Res. **29** (2), 723-37 (2019). DOI: https://doi.org/10.1007/s11053-019-09503-7

[17] R.G. Yu, Z.H. Zhang, W.L. Gao, C.H Li, C. Wu, Numerical simulation of rock mass blasting vibration using particle flow code and particle expansion loading algorithm. Simul. Model. Pract. Th. **122** (2023).
DOI: https://doi.org/10.1016/j.simpat.2022.102686

[18] L. He, D.W. Zhong, Y.H. Liu, K. Song, Prediction of Bench Blasting Vibration on Slope and Safety Threshold of Blasting Vibration Velocity to Undercrossing Tunnel. Shock. Vib. **2021** (1) (2021).
DOI: https://doi.org/10.1155/2021/9939361

[19] Y. Liu, L. Weng, Z.F. Chu, Numerical investigation of rock dynamic fragmentation during rockslides using a coupled 3D FEM-DEM method. J. Mt. Sci-Engl **19** (4), 1051-69 (2022).
DOI: https://doi.org/10.1007/s11629-021-6930-0

[20] M. Lak, M.F. Marji, A.Y. Bafghi, A. Abdollahipour, Discrete element modeling of explosion-induced fracture extension in jointed rock masses. J. Min. Environ. **10**, 125-38 (2019).
DOI: https://doi.org/10.22044/jme.2018.7291.1579

[21] X.F. Huo, Y.J. Jiang, W.P. Wei, X.Y. Qiu, Z. Yu, J.N. Nong, Q.H. Li, Three-dimensional finite element simulation and reconstruction of jointed rock masses for bench blasting. Simul. Model. Pract. Th. **135** (2024).
DOI: https://doi.org/10.1016/j.simpat.2024.102975

[22] V. Kuznetsov, The mean diameter of the fragments formed by blasting rock. Sov. Min. Sci. **9**, 144-8 (1973).
DOI: https://doi.org/10.1007/BF02506177

[23] C. Cunningham, The Kuz-Ram model for prediction of fragmentation from blasting; proceedings of the Proc, first int, symp, on rock fragmentation by blasting. In Proc. first int. symp. on rock fragmentation by blasting (1983).

[24] F. Ouchterlony, J.A. Sanchidrián, A review of the development of better prediction equations for blast fragmentation. J. Rock. Mech. Geotech. **2018**, 25-45 (2018).
DOI: https://doi.org/10.1016/j.jrmge.2019.03.001

[25] F. Bahloul, A. Hafsaoui, A. Idres, Influence of the rock mass structure and the blasting technique on blast results in the heliopolis quarry. Sci. Bull. University **2024** (1), 20-25 (2024).
DOI: https://doi.org/10.33271/nvngu/2024-1/020

[26] Y. Cheikhaoui, H. Cheniti, I. Zeriri, Analyzing Pillar Strength and Behavior using Wolfram Mathematica code: Effects of Cracks, Size and Discretization. Acta. Montan. Slovaca. **29** (3), 604-617 (2024). DOI:https://doi.org/10.46544/AMS.v29i3.08

[27] W. Riedel, N. Kawai, K.I. Kondo, Numerical assessment for impact strength measurements in concrete materials. Int. J. Impact. Eng. **36** (2), 283-93 (2009). DOI: https://doi.org/10.1016/j.ijimpeng.2007.12.012

[28] C. Pan, L.X. Xie, X. Li, K Liu, P.F. Gao, L.G. Tian, Numerical investigation of effect of eccentric decoupled charge structure on blasting-induced rock damage. J. Cent. South. Univ. **29** (2), 663-79 (2022). DOI: https://doi.org/10.1007/s11771-022-4947-3

[29] R.L. Shan, Y. Zhao, H. Wang, Z.F. Liu, H.F. Qin., Blasting vibration response and safety control of mountain tunnel. B. Eng. Geol. Environ. **82** (5), (2023). DOI: https://doi.org/10.1007/s10064-023-03199-z

[30] K.M. Norén-Cosgriff, N. Ramstad, A. Neby, C. Madshus, Building damage due to vibration from rock blasting. Soil. Dyn. Earthq. Eng. **138** (2020). DOI: https://doi.org/10.1016/j.soildyn.2020.106331